Journal of Mathematical Modeling
Vol. 8, No. 1, 2020, pp. 71-90

JMM

The evolution of the free boundary separating two immiscible viscous fluids in an elastic porous medium

Oleg Vladimirovich Galtsev*

Department of Information and Robotic Systems,
Belgorod State National Research University, Belgorod, Russia

Email: galtsev_o@bsu.edu.ru

Abstract. We consider the evolution of the free boundary separating two immiscible viscous fluids with different constant densities in an elastic porous skeleton. The motion of the liquids is described by the Stokes equations driven by the input pressure and the force of gravity. For flows in a bounded domain, we emphasize the study of the properties of the moving boundary separating the two fluids.

Keywords: Hydrodynamic modeling, fluid flows, fluid-structure interaction.
AMS Subject Classification: 76S05, 76D27.

1 Introduction

As a pore space let us consider isolated parallel capillaries $\Pi = \{-l < x_1^{'} < l, -L < x_2^{'} < L\}$ (Fig. 1)which are periodically repeated in the rectangle target domain Ω with sufficiently small l (ideal soil). Let Ω_f and Ω_s, respectively, be the domains occupied by the pore space and the solid skeleton and $\Omega_f^+(t)$, and $\Omega_f^-(t)$ be the subdomains Ω_f, occupied, respectively, by the fluid 1 and the fluid 2.

If μ^+, ρ_f^+ and μ^-, ρ_f^- are the densities and viscosities of fluids, the displacement of fluids in the domains $\Omega_f^{\pm}(t)$ are described by the system of

*Corresponding author.
Received: 31 October 2019 / Revised: 4 January 2020 / Accepted: 8 January 2020.
DOI: 10.22124/jmm.2020.14831.1349

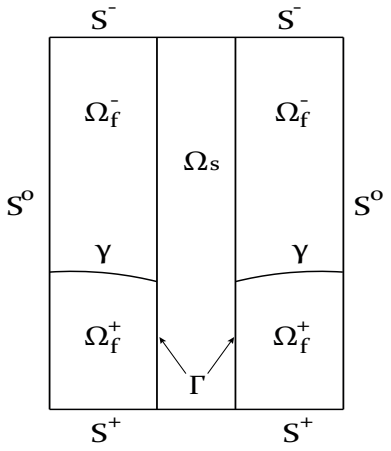

Figure 1: Parallel capillaries

Stokes equations

$$\nabla \cdot \left(\alpha_{\mu^\pm}\, \mathbb{D}(x, \mathbf{v}^\pm) - p_f^\pm\, \mathbb{I}\right) + \rho_f^\pm \mathbf{g} = 0,$$

$$\nabla \cdot \mathbf{v}^\pm = 0,$$

for the velocity $\mathbf{v}^\pm$ and pressure p.

On the free boundary $\gamma(t)$ fluid velocities and the normal stresses are continuous

$$\mathbf{v}^+ = \mathbf{v}^-,$$

$$\left(\alpha_{\mu^+}\, \mathbb{D}(x, \mathbf{v}^+) - p_f^+\, \mathbb{I}\right) \cdot \mathbf{n} = \left(\alpha_{\mu^-}\, \mathbb{D}(x, \mathbf{v}^-) - p_f^-\, \mathbb{I}\right) \cdot \mathbf{n}, \tag{1}$$

where $\mathbf{n}$ is the normal vector to the free surface.

The condition of the material interface $\gamma(t)$ allows us to consider a joint motion of two fluids as the displacement of a non-homogeneous fluid with variable density and viscosity, that do not change along the particles' paths. Differential equations of the motion have the form

$$\nabla \cdot \left(\alpha_\mu\, \mathbb{D}(x, \mathbf{v}) - p_f\, \mathbb{I}\right) + \rho_f \mathbf{g} = 0, \tag{2}$$

$$\nabla \cdot \mathbf{v} = 0, \tag{3}$$

$$\frac{\partial \rho_f}{\partial t} + \nabla \cdot (\rho_f \mathbf{v}) = \frac{\partial \rho_f}{\partial t} + \mathbf{v} \cdot \nabla \rho_f = 0,$$

where $\mathbf{v} = \mathbf{v}^\pm$, $\rho_f = \rho_f^\pm$, $p_f = p_f^\pm$ in $\Omega_f^\pm$.

Displacement of the medium in the solid skeleton Ω_s are described by the Lamé equations

$$\nabla \cdot \left(\alpha_\lambda \, \mathbb{D}(x, \mathbf{w}_s) - p_s \, \mathbb{I}\right) + \rho_s \mathbf{g} = 0, \tag{4}$$

$$\nabla \cdot \mathbf{w}_s = 0. \tag{5}$$

We have the usual conditions of continuity for the velocity vector in the continuous medium and normal stresses on the boundary Γ ("solid skeleton-pore space")

$$\frac{\partial \mathbf{w}_s}{\partial t} = \mathbf{v}, \tag{6}$$

$$\left(\alpha_\lambda \, \mathbb{D}(x, \mathbf{w}_s) - p_s \, \mathbb{I}\right) \cdot \mathbf{n} = \left(\alpha_\mu \, \mathbb{D}(x, \mathbf{v}) - p_f \, \mathbb{I}\right) \cdot \mathbf{n}. \tag{7}$$

This statement is generalized, because it allows us to write the equations of motion in the form of integral identities which do not include the concept of a free boundary between two fluids.

In fact, it is sufficient to determine $\mathbf{w}_f$ and $\mathbf{w}_s$ as

$$\frac{\partial \mathbf{w}_f}{\partial t} = \mathbf{v}, \;\; \mathbf{w} = \mathbf{w}_f \;\in \Omega_f, \;\; \mathbf{w} = \mathbf{w}_s \;\in \Omega_s.$$

Let us multiply equation (2) and (4) by an arbitrary smooth function φ and integrate the results by parts respectively in Ω_f and Ω_s. Then sum results

$$\int_\Omega \Big(\left(\chi \, \alpha_\mu \, \mathbb{D}(x, \frac{\partial \mathbf{w}}{\partial t}) + (1-\chi)\alpha_\lambda \, \mathbb{D}(x, \mathbf{w}) - p \, \mathbb{I}\right) : \\ \mathbb{D}(x, \varphi) - \rho \mathbf{g} \cdot \varphi \Big) dx = 0. \tag{8}$$

Here $\rho = \rho_f \chi + \rho_s (1-\chi)$, $p = p_f \chi + p_s (1-\chi)$. The integrals over the boundary Γ are lost due to boundary conditions (6) and (7).

The differential form of equation (8) has the form

$$\nabla \cdot \left(\chi \, \alpha_\mu \, \mathbb{D}(x, \frac{\partial \mathbf{w}}{\partial t}) + (1-\chi)\alpha_\lambda \, \mathbb{D}(x, \mathbf{w}) - p \, \mathbb{I}\right) + \rho \mathbf{g} = 0. \tag{9}$$

The equation of motion (9) is supplemented by the continuity equation

$$\nabla \cdot \mathbf{w} = 0,$$

which obviously follows from (3) and (5).

The basic equation for an elastic body is written in the *Lagrangian* formulation:

$$\rho \frac{\partial \mathbf{v}}{\partial t} - \nabla \cdot (2\lambda \, \mathbb{D}(\mathbf{w}) - p\mathbb{I}) + \rho \mathbf{g} = 0, \mathbf{x} \in \Omega_s, \tag{10}$$

where $\mathbf{v}$ is the velocity field and $\mathbb{D}(\mathbf{w})$ is the symmetric second order tensor [17]

$$\mathbb{D}(\mathbf{w}) = \frac{1}{2}\left(\nabla'\mathbf{w} + (\nabla'\mathbf{w})^T\right).$$

To close the system of equations we require speed and displacement conditions for the second term:

$$\frac{\partial \mathbf{w}}{\partial t} - \mathbf{v} = 0, \quad \mathbf{x} \in \Omega_s, \tag{11}$$

Inserting (11) into (10), we obtain the equation for $\mathbf{w}$

$$\rho\frac{\partial^2 \mathbf{w}}{\partial t^2} - \nabla \cdot (2\lambda\mathbb{D}(\mathbf{w}) - p\mathbb{I}) + \rho\mathbf{g} = 0, \mathbf{x} \in \Omega_s. \tag{12}$$

In Ω_s the displacement of elastic skeleton $\mathbf{w}_s$ and the pressure p_s satisfy the Lamé equations (1) and (2) on the boundary Γ with conditions (6) and (7).

A two-phase flow can be realized in various ways, for example by establishing a liquid level (level-set method). The transport equation is solved as

$$\frac{\partial \phi}{\partial t} + \mathbf{v} \cdot \nabla\phi = 0, \ x \in \Omega_f, \tag{13}$$

where ϕ is the transport function. The method for establishing the level of the interface between two fluids is determined as a specified isosurface. Therefore at each time a step phase in each computational cell is determined by comparing a simple scalar.

The condition (7) with surface tension takes the form

$$\left((\mathbb{D}(\mathbf{v}^+) - \mathrm{p}^+\mathbb{I}) \cdot \mathbf{n} - (\mathbb{D}(\mathbf{v}^-) - \mathrm{p}^-\mathbb{I}) \cdot \mathbf{n}\right) = \frac{\sigma}{\mathrm{R}}\mathbf{l}, \quad \mathbf{x} \in \gamma(t), \tag{14}$$

where $\mathbf{n}$ is the unit normal to $\gamma(t)$, R is the curvature radius, $\mathbf{l}$ is the unit tangent vector to the interface, σ is the surface tension and (14) coincides with the boundary condition (1) in the absence of surface tension ($\sigma = 0$).

The system of equations (2)–(7) and (13) is supplemented by boundary conditions

$$(2\mu\mathbb{D}(\mathbf{v}) - p\mathbb{I})\mathbf{n} = -p^{\pm}\mathbf{n}, \ \mathbf{x} \in S^{\pm}, \tag{15}$$

$$(2\mu\mathbb{D}(\mathbf{v}) - p\mathbb{I})\mathbf{n} = (\lambda\mathbb{D}(\mathbf{w}) - p\mathbb{I})\mathbf{n}, \ \mathbf{x} \in \Gamma, \tag{16}$$

$$\mathbf{v}^f \cdot \mathbf{n} = 0; \ \mathbf{n} \cdot (2\mu\mathbb{D}(\mathbf{v}^f) - p^f\mathbb{I})\mathbf{n} = 0, \ \mathbf{x} \in S^0, \tag{17}$$

$$\mathbf{w}|_{t=0} = 0, \ \mathbf{x} \in \Omega; \ \mathbf{v}|_{t=0} = 0, \ \mathbf{x} \in \Omega; \ \varphi|_{t=0} = 0, \ \mathbf{x} \in \Omega_f, \tag{18}$$

where S^0 is the boundary of symmetry.

2 ALE-formulation

For the numerical solution of the problem of the joint motion of a fluid and an elastic body we used both formulations: as two functions $(\mathbf{w}, \mathbf{v})$ – equations (10), (11), and as a single function $(\mathbf{w})$ – equation (12) (see [16], [12]).

Here are two formulations of the equations for the fluid component. The first is the Eulerian (natural) fluid description, the second is a free Lagrangian-Eulerian formulation (ALE-formulation). The ALE-description is necessary to simulate fluid-structure interaction and allows us to link the boundary conditions between the fluid and the elastic body.

For a viscous incompressible fluid the system of equations consists of Stokes equations in the Euler formulation are:

$$\rho\frac{\partial \mathbf{v}}{\partial t} - \nabla \cdot (2\mu\,\mathbb{D}(\mathbf{v}) - p\mathbb{I}) + \rho\mathbf{g} = 0, \mathbf{x} \in \Omega_f(t), \tag{19}$$

where $\Omega_f(t)$ is the current fluid deformable area, $\mathbf{v}$ is the fluid velocity field, p is the pressure, μ is the viscosity, and $\mathbb{D}(\mathbf{v})$ is the symmetric second order tensor

$$\mathbb{D}(\mathbf{v}) = \frac{1}{2}\left(\nabla\mathbf{v} + (\nabla\mathbf{v})^T\right)$$

and the condition of incompressibility is

$$\nabla \cdot \mathbf{v} = 0,\ \mathbf{x} \in \Omega_f(t). \tag{20}$$

As previously mentioned, the arbitrary Lagrangian-Euler formulation is needed to describe the fluid-structure interaction in a single system. For this we rewrite the equations (19) and (20), using the following relations:

$$\nabla\mathbf{v} = \nabla'\mathbf{v}_k\mathbf{F}^{-1}$$

and

$$\frac{\partial \mathbf{v}}{\partial t} = \frac{\partial \mathbf{v}_k}{\partial t} - \mathbf{v}_f \cdot (\nabla'\mathbf{v}_k\mathbf{F}^{-1}),$$

where k is the index denoting the variables in the ALE formulation, $\mathbf{v}_f$ is the fluid velocity field, which is defined as $\mathbf{v}_f = \partial\chi/\partial t$. The deformation gradient is defined as

$$\mathbf{F} = \nabla'\mathbf{w} + \mathbb{I},$$

where $\mathbb{I}$ is the identity tensor, ∇' denote differential operators with respect to the start position $\mathbf{X}$ of a material point. Motion defined as

$$\chi(\mathbf{X}, t) = \mathbf{X} + \mathbf{w},$$

$$\mathbf{w} = \mathbf{x}(\mathbf{X}, t) - \mathbf{X}.$$

Thus equation (19) takes the form:

$$\rho \frac{\partial \mathbf{v}_k}{\partial t} - \nabla \cdot (2\mu\, \mathbb{D}(\mathbf{v}_k) - p_k \mathbb{I}) + \rho \mathbf{g}_k = 0, \mathbf{X} \in \Omega_f(0), \tag{21}$$

and

$$(F^{-1} : \nabla' \mathbf{v}_k^T) = 0, \ \mathbf{X} \in \Omega_f(0), \tag{22}$$

where $\Omega_f(0)$ is the region being considered that is occupied by the fluid. The stress tensor is:

$$\mathbb{D}(\mathbf{v}_k) = \frac{1}{2}\left(\nabla' \mathbf{v}_k \mathbf{F}^{-1} + \mathbf{F}^{-T}(\nabla' \mathbf{v}_k)^T\right).$$

Now when the system of Stokes equations is written in an arbitrary Lagrangian-Euler formulation, it is possible to combine it with the equations for an elastic body and solve the problem of fluid-structure interaction.

For equation (13), as well as for equation (21) the required ALE-formulation to find values in the calculated deformed area is:

$$\frac{\partial \phi}{\partial t} + (\mathbf{v}_k - \mathbf{v}_f) \cdot \nabla \phi = 0, \ \mathbf{X} \in \Omega_f, \tag{23}$$

where $\mathbf{v}_f = (x(t_{n+1}) - x(t_n))/\Delta t$ is the velocity of computational mesh and Δt is the time step.

It should be noted that the equations (21), (22) and (23) are a coupled system where there is a mutual influence of the level-set function on the liquid velocity. If there is an elastic body as a third phase, then the fluid will affect the displacement of the elastic body, and the body in turn will act on the fluid subdomain (Fig. 2).

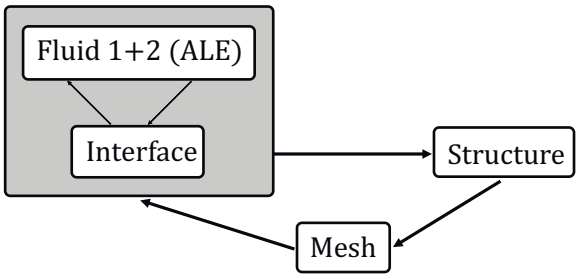

Figure 2: Interaction of the two-phase liquid components and elastic body

The determinant of $\mathbf{F}$ is

$$J = det(\mathbf{F}).$$

3 Finite element method

There are several methodologies for solving the partial differential equations (PDE) described above. Some of the more common methods are the finite element method (FEM), the finite volume method (FVM), and the discontinuous Galerkin method (DGM). Although all of these methods can be used for any PDE, and therefore work for both solid and fluid analysis, FEM is typically used to analyze solids, while FVM and DGM are more commonly used for fluid analysis.

The finite volume method divides the computational domain into a finite number of locally-conservative control volumes centered about a node. All of the quantities for a control volume are calculated at this node, so they have to be interpolated to the volume's surface. The finite volume method is locally- and globally-conservative as long as consistent surface integrals, which correspond with convective and diffusive fluxes, are used between neighboring control volumes and the domain boundary [4], [18]. The fact that mass and other properties are conserved through each volume makes FVM ideal for CFD; unfortunately, as all calculations are for the volume as a whole, FVM is inherently poor at structural analysis, where localized stresses could occur at locations poorly represented by the control point.

Instead of breaking the domain up into node centered volumes, the finite element method divides the domain into individual elements which contain basis functions. Basis functions are members of a function space, such as polynomials, which approximate the values a quantity has inside the element [1]. Basis functions allow for interpolation of data at any point inside the element, which makes FEM desirable for structural analysis [9, 10]. As the computational ability of computers has increased, FEM has been growing in popularity for use in CFD as well.

The discontinuous Galerkin method is unique in that it has the benefits of both FEM and FVM. DGM uses basis functions inside the element, like FEM, but it couples neighboring elements through fluxes, like FVM. This leads to it being locally conservative, stable, and high-order accurate while also allowing for complex geometries, irregular meshes with hanging nodes, and approximations that have polynomials of different degrees in different elements [2]. However, due to its perceived computational cost, DGM is less frequently used than FEM or FVM.

Due to the desire to provide both partitioned and monolithic fluid-structure interaction coupling, a unified framework is required for the solid and fluid formulations in this research. This not only entails the ALE description discussed in the previous section, but also a unified solution method. Based on the discussion above, along with more reasons men-

tioned in the following section, the finite element method was chosen as the solution technique (see [6,11,15,19]). The weighted residuals method is used to convert differential equations in integral form (weak formulation). The spatial discretization of a weak formulation allows one to obtain a system of ordinary differential equations in time (semi-discrete form). Time discretization of semi-discrete equations leads to a fully discrete system of algebraic equations. If this is non-linear, it must be linearized.

All of the governing equations presented necessitate second derivatives in their current form, which can be very difficult to solve. According to the numerical method, it is necessary to rewrite the original system of equations in a weak formulation. To do this, multiply our equations by an arbitrary weight function such that $\hat{\mathbf{u}} \in H^1_\Gamma = \{\hat{\mathbf{u}} \in L^2,\ \hat{\mathbf{u}}|_\Gamma = 0\}$ and integrate each term (see [3]).

Thus, the weak form of the equations of elasticity will be as follows:

$$\int_{\Omega_s} \rho \frac{\partial^2 \mathbf{w}}{\partial t^2} \cdot \hat{\mathbf{w}} - \int_{\Omega_s} div\,(2\mu\,\mathbb{D}(\mathbf{w}) - p\mathbb{I}) \cdot \hat{\mathbf{w}} - \int_{\Omega_s} \rho \mathbf{g} \cdot \hat{\mathbf{w}} = 0. \tag{24}$$

Using integration by parts, the stress tensor takes the form:

$$\int_{\Omega_s} div\,(2\mu\,\mathbb{D}(\mathbf{w}) - p\mathbb{I}) \cdot \hat{\mathbf{w}} = \int_{\partial\Omega_s} \mathbf{t} \cdot \hat{\mathbf{w}} - \int_{\Omega_s} (\mathbb{D}(\mathbf{w}) - p\mathbb{I}) \cdot \nabla \hat{\mathbf{w}}, \tag{25}$$

where $\mathbf{t} \equiv (\mathbb{D}(\mathbf{w}) - p\mathbb{I}) \cdot \mathbf{n}$. Inserting (25) into (24) we obtain:

$$\int_{\Omega_s} \rho \frac{\partial^2 \mathbf{w}}{\partial t^2} \cdot \hat{\mathbf{w}} + \int_{\Omega_s} (2\mu\,\mathbb{D}(\mathbf{w}) - p\mathbb{I}) : \mathbb{D}(\hat{\mathbf{w}}) - \int_{\Omega_s} \rho \mathbf{g} \cdot \hat{\mathbf{w}} - \int_{\partial\Omega_s} \mathbf{t} \cdot \hat{\mathbf{w}} = 0,$$

and perform the same procedure for (10) and (11), taking the weight functions $\hat{\mathbf{v}}$ of velocities and $\hat{\mathbf{w}}$ of displacements respectively:

$$\int_{\Omega_s} \rho \frac{\partial \mathbf{v}}{\partial t} \cdot \hat{\mathbf{v}} + \int_{\Omega_s} (2\mu\,\mathbb{D}(\mathbf{w}) - p\mathbb{I}) : \mathbb{D}(\hat{\mathbf{v}}) - \int_{\Omega_s} \rho^s \mathbf{g} \cdot \hat{\mathbf{v}} - \int_{\partial\Omega_s} \mathbf{t} \cdot \hat{\mathbf{v}} = 0, \tag{26}$$

$$\int_{\Omega^s} \frac{\partial \mathbf{w}}{\partial t} \cdot \hat{\mathbf{w}} - \int_{\Omega^s} \mathbf{v} \cdot \hat{\mathbf{w}} = 0, \tag{27}$$

The weak formulation of the Stokes equations will have the form:

$$\int_{\Omega_f} \rho \frac{\partial \mathbf{v}}{\partial t} \cdot \hat{\mathbf{v}} + \int_{\Omega_f} 2\mu \mathbb{D}(\mathbf{v}) : \mathbb{D}(\hat{\mathbf{v}}) - \int_{\Omega_f} p\, div\, \hat{\mathbf{v}} = \int_{\Omega_f} \rho \mathbf{g} \cdot \hat{\mathbf{v}} + \int_{\partial\Omega_f} \mathbf{t} \cdot \hat{\mathbf{v}},$$

$$\int_{\Omega_f} \hat{p}\, div\, \mathbf{v} = 0,$$

where $\hat{p}$ is the weight function of pressure.

The ALE-formulation will be the same, but it is necessary to consider the transition from Euler form to ALE form

$$\int_{\Omega_f(t)} f(\mathbf{x})\,dx = \int_{\Omega_f(0)} f_k(\mathbf{X})\,dX.$$

Further $\Omega_f \equiv \Omega_f(0)$. Taking the same weight function, as well as for the formulation of the Euler equations, we obtain the weak formulation of the equation(21) and (22)

$$\int_{\Omega_f} J\rho\frac{\partial \mathbf{v}_k}{\partial t}\cdot\hat{\mathbf{v}} + \int_{\Omega_f} J(2\mu\mathbb{D}(\mathbf{v}_k) - p_k\mathbb{I})\mathbf{F}^{-T} : \mathbb{D}(\hat{\mathbf{v}}) - \int_{\Omega_f} J\rho\mathbf{g}_k\cdot\hat{\mathbf{v}} - \int_{\partial\Omega_f} J\mathbf{t}_k\cdot\hat{\mathbf{v}} = 0,$$

$$\int_{\Omega_f} (J\mathbf{F}^{-1} : \nabla'\mathbf{v}_k^T)\cdot\hat{p} = 0.$$

4 Finite element spatial discretization

The meaning of digitization is to divide the area into separate limited piecewise continuous subregions. The set of these elements is defined as a mesh, which is a model of the original area. The basic variables are the approximated nodal values multiplied by the basis vector, which is required for interpolation within the cell. Our approximation will be as follows:

$$\mathbf{w} \approx \sum_{j=1}^{n} \hat{\mathbf{w}}_j W_j, \quad \mathbf{v} \approx \sum_{j=1}^{n} \hat{\mathbf{v}}_j V_j, \quad p \approx \sum_{j=1}^{n} \hat{p}_j P_j,$$

where $\hat{\mathbf{w}}_j, \hat{\mathbf{v}}_j$ and $\hat{p}_j$ are j-th basis vectors, n is the number of nodes, W_j, V_j and P_j are j-th values at the nodes associated with the primary variables. The set of basis vectors is taken as a set of weighted vectors. Thus the weighted function can be determined as follows:

$$\hat{\mathbf{w}} = \sum_{i=1}^{n} \hat{\mathbf{w}}_i W_i,\ \hat{\mathbf{v}} = \sum_{i=1}^{n} \hat{\mathbf{v}}_i V_i,\ \hat{p} = \sum_{i=1}^{n} \hat{p}_i P_i.$$

Nodal values associated with weighted functions are arbitrary, so they can be ignored.

5 Finite element time discretization

Finite differences are used to approximate our equations. The general equation after the spatial discretization will be as follows:

$$\frac{d\mathbf{v}(t)}{dt} = g(t).$$

Integrating both sides over time we get:

$$\int_{t_n}^{t_{n+1}} \frac{d\mathbf{v}(t)}{dt} dt = \int_{t_n}^{t_{n+1}} g(t)dt.$$

The first integral can be written as

$$\int_{t_n}^{t_{n+1}} \frac{d\mathbf{v}(t)}{dt} dt = \mathbf{v}^{n+1} - \mathbf{v}^n,$$

the second integral can be approximated by using only the average value for a certain time τ

$$\int_{t_n}^{t_{n+1}} g(t)dt \approx g(\tau)\Delta t,$$

where $t_n \leq \tau \leq t_{n+1}$. Then the explicit left and right implicit Euler approximation will have the form:

$$\frac{\mathbf{v}^{n+1} - \mathbf{v}^n}{\Delta t} = g(t_{n+1}), \quad \frac{\mathbf{v}^{n+1} - \mathbf{v}^n}{\Delta t} = g(t_n).$$

To combine the left and right sides in Euler's method, we use the θ-method:

$$\frac{\mathbf{v}^{n+1} - \mathbf{v}^n}{\Delta t} = \theta g(t_{n+1}) + (1 - \vartheta) g(t_n),$$

where $\theta = 1$ or $\theta = 0$. The special case, when $\theta = 0.5$, can be approximated as:

$$\frac{\mathbf{v}^{n+1} - \mathbf{v}^n}{\Delta t} = 0.5 \left(g(t_{n+1}) + g(t_n) \right),$$

to satisfy the second order condition of accuracy with respect to time.

Using the θ-method, rewrite the equations (26) and (27) as follows:

$$\int_{\Omega_s} \rho \frac{\mathbf{v}^{n+1} - \mathbf{v}^n}{\Delta t} \cdot \hat{\mathbf{v}} = \theta \left(- \int_{\Omega_s} \mathbf{T}_R^{n+1} \cdot \hat{\mathbf{v}} + \int_{\partial\Omega_s} \mathbf{t}^{n+1} \cdot \hat{\mathbf{v}} \right) + (1 - \theta) \left(- \int_{\Omega_s} \mathbf{T}_R^{n} \cdot \hat{\mathbf{v}} + \int_{\partial\Omega_s} \mathbf{t}^{n} \cdot \hat{\mathbf{v}} \right),$$

$$\int_{\Omega_s} \rho \frac{\mathbf{w}^{n+1} - \mathbf{w}^n}{\Delta t} \cdot \hat{\mathbf{w}} = \theta \int_{\Omega_s} \mathbf{v}^{n+1} \cdot \hat{\mathbf{w}} + (1 - \theta) \int_{\Omega_s} \mathbf{v}^{n} \cdot \hat{\mathbf{w}},$$

where $\mathbf{T}_R = 2\mu\mathbb{D}(\mathbf{v}) - p\mathbb{I}$.

The time derivatives for other governing equations are handled with the θ-method. For brevity, we will not write it here.

6 Fluid-structure interaction

The system of equations for a fluid-structure interaction arises by finding the residuals of the discretized governing equations (the discretization error) and taking a Taylor series expansion of these residuals (see [8], [14]).

In the appropriate Jacobians, residuals, and unknowns, the monolithic system of equations can be written as

$$\begin{bmatrix} \mathbf{J}_{w_s w_s} & \mathbf{J}_{w_s v_s} & \mathbf{J}_{w_s v_f} & \mathbf{J}_{w_s p_f} & \mathbf{J}_{w_s w_m} \\ \mathbf{J}_{v_s w_s} & \mathbf{J}_{v_s v_s} & \mathbf{J}_{v_s v_f} & \mathbf{J}_{v_s p_f} & \mathbf{J}_{v_s w_m} \\ \mathbf{J}_{v_f w_s} & \mathbf{J}_{v_f v_s} & \mathbf{J}_{v_f v_f} & \mathbf{J}_{v_f p_f} & \mathbf{J}_{v_f w_m} \\ \mathbf{J}_{p_f w_s} & \mathbf{J}_{p_f v_s} & \mathbf{J}_{p_f v_f} & \mathbf{J}_{p_f p_f} & \mathbf{J}_{p_f w_m} \\ \mathbf{J}_{w_m w_s} & \mathbf{J}_{w_m v_s} & \mathbf{J}_{w_m v_f} & \mathbf{J}_{w_m p_f} & \mathbf{J}_{w_m w_m} \end{bmatrix} \begin{bmatrix} \mathbf{W}_s \\ \mathbf{V}_s \\ \mathbf{V}_f \\ \mathbf{P}_f \\ \mathbf{W}_m \end{bmatrix} = - \begin{bmatrix} \mathbf{R}_{w_s} \\ \mathbf{R}_{v_s} \\ \mathbf{R}_{v_f} \\ \mathbf{R}_{p_f} \\ \mathbf{R}_{w_m} \end{bmatrix},$$

where the variables of the elastic component are denoted by index s, the fluid component by f, and the mesh variables are m. The nonlinear terms are linearized using the Newton-Raphson method, based on the definition of a Jacobian (see [5]):

$$\mathbf{J}_{hk} \equiv \frac{\partial \mathbf{R}_h}{\partial \mathbf{K}}, \tag{28}$$

where $\mathbf{R}_h$ is the h-th residual and $\mathbf{K}$ is some unknown.

This system is obtained by finding the residuals of the discretized equations (sampling error) and using a Taylor series expansion of these residuals.

A solid body is studied using two variables in the elasticity equations, where the residuals are found as

$$R^i_{w_s} = \int_{\Omega_s} \frac{\partial \mathbf{w}_s}{\partial t} \cdot \hat{\mathbf{w}}^i_s - \int_{\Omega_s} \mathbf{v}_s \cdot \hat{\mathbf{w}}^i_s,$$

$$R^i_{v_s} = \int_{\Omega_s} \rho_s \frac{\partial \mathbf{v}_s}{\partial t} \cdot \hat{\mathbf{v}}^i_s + \int_{\Omega_s} (2\mu\, \mathbb{D}(\mathbf{w}_s) - p\mathbb{I}) : \mathbb{D}(\hat{\mathbf{v}}^i_s) - \int_{\Gamma} \mathbf{t}_s \cdot \hat{\mathbf{v}}^i_s.$$

The position of the border "fluid-elastic body" is defined by the normal stress

$$\mathbf{t}_s = \left(2\mu(\nabla' \mathbf{v}_k \mathbf{F}^{-1} + \mathbf{F}^{-T} \nabla' \mathbf{v}_k^T) - p_k \mathbb{I}\right) \cdot \left(J\mathbf{F}^{-T}\mathbf{n}\right).$$

The fluid is described by the Stokes equations in the ALE-formulation of the following residuals

$$R^i_{v_f} = \int_{\Omega_f} \left(J\, \rho_f \frac{\partial \mathbf{v}_k}{\partial t} \cdot \hat{\mathbf{v}}^i_f \right) + \int_{\Omega_f} \left(J(2\mu(\nabla' \mathbf{v}_k \mathbf{F}^{-1} + \mathbf{F}^{-T} \nabla' \mathbf{v}_k^T) - p_k \mathbb{I})\mathbf{F}^{-T} \right) \nabla' \hat{\mathbf{v}}^i_f,$$

and

$$R^i_{p_f} = \int_{\Omega_f} (J\mathbf{F}^{-1} : \nabla' \mathbf{v}_k^T) \cdot \hat{p}^i,$$

where index k indicates affiliation to the ALE field.

The residuals for the computational mesh are

$$R^i_{w_m} = \int_{\Omega_f} \mu(\nabla' \mathbf{w}_m + \nabla' \mathbf{w}_m^T)\nabla' \hat{\mathbf{w}}^i_m + \int_{\Omega_f} \lambda(\nabla' \cdot \mathbf{w}_m)\, \nabla' \cdot \hat{\mathbf{w}}^i_m.$$

All of the residuals from equation (6) are now defined. Using these definitions and applying equation (28), we can determine the Jacobians. In the monolithic formulation many Jacobians are equal to zero in the overall system:

$$\begin{bmatrix} \mathbf{J}_{w_s w_s} & \mathbf{J}_{w_s v_s} & 0 & 0 & 0 \\ \mathbf{J}_{v_s w_s} & \mathbf{J}_{v_s v_s} & \mathbf{J}_{v_s v_f} & \mathbf{J}_{v_s p_f} & \mathbf{J}_{v_s w_m} \\ 0 & 0 & \mathbf{J}_{v_f v_f} & \mathbf{J}_{v_f p_f} & \mathbf{J}_{v_f w_m} \\ 0 & 0 & \mathbf{J}_{p_f v_f} & 0 & \mathbf{J}_{p_f w_m} \\ 0 & 0 & 0 & 0 & \mathbf{J}_{w_m w_m} \end{bmatrix} \begin{bmatrix} \mathbf{W}_s \\ \mathbf{V}_s \\ \mathbf{V}_f \\ \mathbf{P}_f \\ \mathbf{W}_m \end{bmatrix} = - \begin{bmatrix} \mathbf{R}_{w_s} \\ \mathbf{R}_{v_s} \\ \mathbf{R}_{v_f} \\ \mathbf{R}_{p_f} \\ \mathbf{R}_{w_m} \end{bmatrix},$$

For convenience, we denote $()' \equiv \partial()/\partial \mathbf{W}_m$. In assessing the Jacobian the following identities are required [7]:

$$J' = J\, tr(\mathbf{F}' \mathbf{F}^{-1}),$$

$$(\mathbf{F}^{-T})' = \left((\mathbf{F}^{-1})'\right)^T,$$

$$(\mathbf{F}^{-1})' = -\mathbf{F}^{-1}\mathbf{F}'\mathbf{F}^{-1},$$

$$\mathbf{F}' = \nabla' \hat{\mathbf{w}}^j_m.$$

The approximate velocity of the mesh motion in the fluid components like $\mathbf{v}_m \approx (\chi - \chi^n)/\Delta t$, are

$$\mathbf{v}'_m = \frac{\hat{\mathbf{w}}^j_m}{\Delta t}.$$

Jacobians of the solid part will be

$$J^{ij}_{w_s w_s} = \int_{\Omega_s} \frac{\partial \hat{\mathbf{w}}^j_s}{\partial t} \cdot \hat{\mathbf{w}}^i_s,$$

$$J^{ij}_{w_s v_s} = -\int_{\Omega_s} \hat{\mathbf{v}}^j_s \cdot \hat{\mathbf{w}}^i_s,$$

$$J^{ij}_{v_s w_s} = \int_{\Omega_s} \mathbf{T}^j_R \nabla' \hat{\mathbf{v}}^i_s,$$

$$J^{ij}_{v_s v_s} = \int_{\Omega_s} \rho_s \frac{\partial \hat{\mathbf{v}}^j_s}{\partial t} \cdot \hat{\mathbf{v}}^i_s,$$

where

$$\mathbf{T}_R^j = \nabla^{'}\mathbf{w}_s^j\left[2\mu\,\mathbb{D}(\mathbf{w}_s) + p_s\mathbb{I}\right] + (\mathbb{I} + \nabla^{'}\mathbf{w}_s)\left[2\mu\,\mathbb{D}(\hat{\mathbf{w}}_s^j) + p_s\mathbb{I}\right].$$

The Jacobians of the fluid part will be as follows:

$$J_{v_f p_f}^{ij} = -\int_{\Omega_f} J\hat{p}_f^j\mathbf{F}^{-T}\,\nabla^{'}\hat{\mathbf{v}}_f^i,$$

$$J_{p_f v_f}^{ij} = \int_{\Omega_f}(J\mathbf{F}^{-1} : \nabla^{'}\hat{\mathbf{v}}_f^j)\hat{p}^i,$$

$$\begin{aligned}J_{v_f v_f}^{ij} = &\int_{\Omega_f} J\rho_f\frac{\partial\hat{\mathbf{v}}_f^j}{\partial t}\cdot\hat{\mathbf{v}}_f^i + \int_{\Omega_f} J\rho_f\hat{\mathbf{v}}_f^i(\nabla^{'}\mathbf{v}_k\mathbf{F}^{-1})\cdot\hat{\mathbf{v}}_f^j\\ &+\int_{\Omega_f}(J\,2\mu\nabla^{'}\hat{\mathbf{v}}_f^j\mathbf{F}^{-1}\mathbf{F}^{-T})\nabla^{'}\hat{\mathbf{v}}_f^i + \int_{\Omega_f}(J\,2\mu\mathbf{F}^{-T}\nabla^{'}\hat{\mathbf{v}}_f^j\mathbf{F}^{-T})\nabla^{'}\hat{\mathbf{v}}_f^i.\end{aligned}$$

The Jacobian of the computational mesh is

$$J_{w_m w_m}^{ij} = \int_{\Omega_f}\mu(\nabla^{'}\mathbf{w}_m^j + \nabla^{'}\mathbf{w}_m^{j\,T})\nabla^{'}\hat{\mathbf{w}}_m^i + (\lambda(\nabla^{'}\cdot\hat{\mathbf{w}}_m^j)\,\nabla^{'}\cdot\hat{\mathbf{w}}_m^i).$$

And the Jacobians of fluid interaction with the computational mesh will look like:

$$\begin{aligned}J_{v_f w_m}^{ij} = &\int_{\Omega_f} J^{'}\rho_f\frac{\partial\mathbf{v}_k}{\partial t}\cdot\hat{\mathbf{v}}_f^i - \int_{\Omega_f}[J^{'}\rho_f(\nabla^{'}\mathbf{v}_k\mathbf{F}^{-1})(\mathbf{v}_m)]\,\hat{\mathbf{v}}_f^i\\ &-\int_{\Omega_f}[J\rho_f(\nabla^{'}\mathbf{v}_k(\mathbf{F}^{-1})^{'})(\mathbf{v}_m)]\hat{\mathbf{v}}_f^i - \int_{\Omega_f}[J\rho_f(\nabla^{'}\mathbf{v}_k\mathbf{F}^{-1})(\mathbf{v}_m^{'})]\hat{\mathbf{v}}_f^i\\ &+\int_{\Omega_f}[J^{'}\rho_f(\nabla^{'}\mathbf{v}_k\mathbf{F}^{-1})(\mathbf{v}_k)]\hat{\mathbf{v}}_f^i + \int_{\Omega_f}[J\rho_f(\nabla^{'}\mathbf{v}_k(\mathbf{F}^{-1})^{'})(\mathbf{v}_k)]\hat{\mathbf{v}}_f^i\\ &-\int_{\Omega_f}[J^{'}p_k\mathbf{F}^{-T}]\nabla^{'}\hat{\mathbf{v}}_f^i - \int_{\Omega_f}[Jp_k(\mathbf{F}^{-T})^{'}]\nabla^{'}\hat{\mathbf{v}}_f^i\\ &+\int_{\Omega_F}[J^{'}\mu\nabla^{'}\mathbf{v}_k\mathbf{F}^{-1}F^{-T}]\nabla^{'}\hat{\mathbf{v}}_f^i + \int_{\Omega_F}[J\,\mu\nabla^{'}\mathbf{v}_k(\mathbf{F}^{-1})^{'}\mathbf{F}^{-T}]\nabla^{'}\hat{\mathbf{v}}_f^i\\ &+\int_{\Omega_F}(J\,\mu\nabla^{'}\mathbf{v}_k\mathbf{F}^{-1}(\mathbf{F}^{-T})^{'})\nabla^{'}\hat{\mathbf{v}}_f^i + \int_{\Omega_F}[J^{'}\mu\mathbf{F}^{-T}\nabla^{'}\mathbf{v}_k^T\mathbf{F}^{-T}]\nabla^{'}\hat{\mathbf{v}}_f^i\\ &+\int_{\Omega_F}[J\,\mu(\mathbf{F}^{-T})^{'}\nabla^{'}\mathbf{v}_k^T\mathbf{F}^{-T}]\nabla^{'}\hat{\mathbf{v}}_f^i\\ &+\int_{\Omega_F}[J\,\mu\mathbf{F}^{-T}\nabla^{'}\mathbf{v}_k^T(\mathbf{F}^{-T})^{'}]\nabla^{'}\hat{\mathbf{v}}_f^i,\end{aligned}$$

$$J_{p_f w_{ms}}^{ij} = \int_{\Omega_f}^{'}(J^{'}\mathbf{F}^{-1} : \nabla^{'}\mathbf{v}_k^T)\cdot\hat{p}^i + \int_{\Omega_f}(J(\mathbf{F}^{-1})^{'} : \nabla^{'}\mathbf{v}_k^T)\cdot\hat{p}^i,$$

Application of equation (28) implies that there should also be Jacobians $J^{ij}_{v_s v_f}, J^{ij}_{v_s p_f}, J^{ij}_{v_s w_m}$. But these terms appear in the monolithic case, and only as a result of the fluid traction acting on the solid. Velocity continuity is strongly enforced across the interface. This means the velocities are continuous on the interface.

The key point here is that the weight functions must also be continuous, as they are defined using the same basis vectors as for the velocity and displacement. This means that $\hat{\mathbf{v}}_f - \hat{\mathbf{v}}_s \,|_\Gamma = 0$. The rigid body displacement defines an offset mesh on the border of the "liquid-solid body":

$$\mathbf{w}_m - \mathbf{w}_s \,|_\Gamma = 0,$$

and the velocity of the solid state defines the velocity of the fluid at the same border:

$$\mathbf{v}_f - \mathbf{v}_s \,|_\Gamma = 0.$$

7 Error estimation

The method of manufactured solutions [13] is used to verify governing equations. After the exact solution is chosen, the verification is done by examining the error between the exact solution and the approximate solution. Two error norms were considered: L^2 (Hilbert space) and H^1 (Lebesgue space). The errors with respect to these norms are defined over a mesh cell k as

$$\|w - w_h\|_{L^2(k)} = \sqrt{\int_k |w(x) - w_h(x)|^2 dx}, \tag{29}$$

$$\|w - w_h\|_{H^1(k)} = \sqrt{\|w - w_h\|^2_{L^2(k)} + \int_k |\nabla w(x) - \nabla w_h(x)|^2 dx}, \tag{30}$$

where, for this case, $w(x)$ is the exact solution, $w_h(x)$ is the approximate solution.

Thus

$$\|w - w_h\| = c\, h^{\alpha+\beta}, \tag{31}$$

where α is a parameter based on the space of the norm, β is a polynomial order, h is a cell width, c is a constant. Note that error norms in the Hilbert space are optimal when $\alpha = 0$, but in the Lebesgue space when $\alpha = 1$.

This method was applied to the discrete governing equations developed above. For brevity, let us estimate the errors only for the Lame's elasticity equations (10)–(12). The manufactured solution for the displacement $\mathbf{w} = (w_1, w_2)$ is chosen as: $w_1 = 2\sin(2\pi x)\sin(\pi y)\sin(\pi t)$,

Table 1: Error estimation for $Q1$ displacement and velocity elements of the elasticity equations.

cells	$\|w_1 - w_{1\,h}\|_{L^2}$	$\|w_1 - w_{1\,h}\|_{H^1}$
64	2.754E-06	0.621E-04
256	0.504E-06	2.843E-05
1024	1.154E-07	1.840E-05
4056	2.911E-08	0.732E-05
cells	$\|w_2 - w_{2\,h}\|_{L^2}$	$\|w_2 - w_{2\,h}\|_{H^1}$
64	1.812E-06	3.221E-05
256	3.812E-07	1.583E-05
1024	0.753E-07	0.750E-05
4056	1.742E-08	3.720E-06
cells	$\|v_1 - v_{1\,h}\|_{L^2}$	$\|v_1 - v_{1\,h}\|_{H^1}$
64	0.610E00	1.505E01
256	1.251E-01	0.741E01
1024	2.434E-02	3.612E00
4056	0.734E-02	1.825E00
cells	$\|v_2 - v_{2\,h}\|_{L^2}$	$\|v_2 - v_{2\,h}\|_{H^1}$
64	4.753E-01	0.806E01
256	0.948E-03	3.821E00
1024	1.923E-03	1.841E00
4056	4.353E-03	4.605E-01

$w_2 = -\cos(2\pi x)\cos(\pi y)\sin(\pi t)$. The manufactured solution for the velocity $\mathbf{v} = (v_1, v_2)$ is chosen as: $v_1 = 2\pi\sin(2\pi x)\sin(\pi y)\cos(\pi t)$, $v_2 = -\pi\cos(2\pi x)\cos(\pi y)\sin(\pi t)$.

Table 1 shows the error norms for $Q1$ elements. Using equation (31) we can compare to the optimal rate, where the $\alpha+\beta$ is the optimal rate. Here $\beta = 1$. As we can see, the model convergences are optimal. These errors were calculated with a timestep size $\Delta t = 0.0001$.

Following the same procedure as before, we can get error norms for Stokes equations (2) and (3). The manufactured solution for the velocity $\mathbf{v} = (v_1, v_2)$ is

$$v_1 = \sin(4\pi x)\sin(4\pi y)\sin(4\pi t), \quad v_2 = \cos(4\pi x)\cos(4\pi y)\sin(4\pi t),$$

and the pressure p is $p = 4\pi\mu\cos(4\pi x)\sin(4\pi t)\sin(4\pi y)$. $Q2$ elements are used for the velocity and $Q1$ elements are used for the pressure.

8 Numerical experiments

Applying the above algorithms for numerical simulation of fluid-by-fluid displacement in an elastic porous medium, we were able to obtain the dependence of the interface velocity on the Lame's coefficient of elasticity. For all the cases considered below there is a distinctive feature of the free surface behavior.

Numerical simulations indicated that there are differences using various values of the coefficient of elasticity. It is noticeable that with an increased coefficient of elasticity the fluid movement in the capillary is reduced (see Fig. 3–5). The propagation velocity of the free boundary in an elastic porous medium also depends on the surface tension coefficient (see Fig. 6–7).

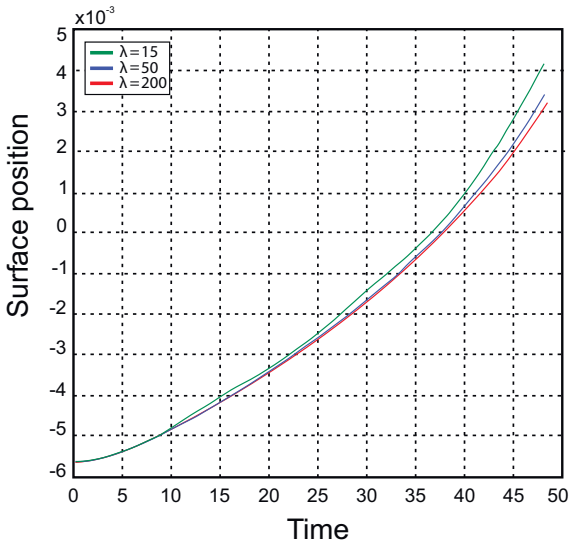

Figure 3: The plot of the free boundary position changes over time for different values of $\lambda = [15; 50; 200]$. Here density $\rho^+ = 1.1$, $\rho^- = 0.86$, viscosities $\mu^+ = 0.001$, $\mu^- = 0.01$, inlet pressure $p^+ = 10$ and surface tension $\sigma = 0$.

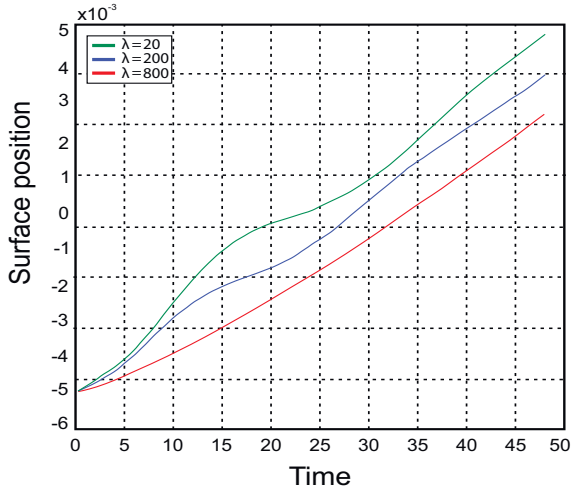

Figure 4: The plot of the free boundary position changes over time for different values of $\lambda = [20; 200; 800]$. Here density $\rho^+ = 1.1$, $\rho^- = 0.86$, viscosities $\mu^+ = 0.001$, $\mu^- = 0.01$, inlet pressure $p^+ = 10$ and surface tension $\sigma = 0.5$.

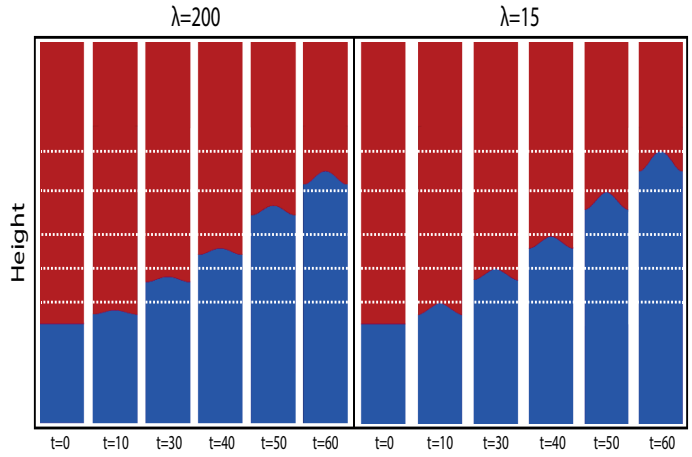

Figure 5: Numerical simulation results for different $\lambda = [15; 200]$ over time. Here density $\rho^+ = 1.1$, $\rho^- = 0.86$, viscosities $\mu^+ = 0.001$, $\mu^- = 0.01$, inlet pressure $p^+ = 10$ and surface tension $\sigma = 0.1$.

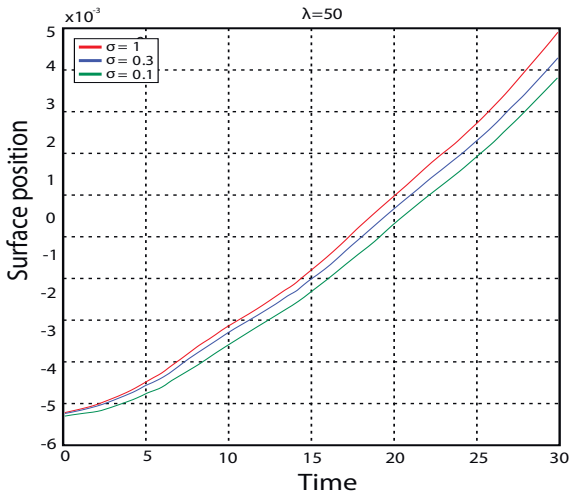

Figure 6: The plot of the free boundary position changes over time for different values of $\sigma = [0.1; 0.3, 1]$. Here density $\rho^+ = 1.1$, $\rho^- = 0.86$, viscosities $\mu^+ = 0.001$, $\mu^- = 0.01$, inlet pressure $p^+ = 10$ and Lame's coefficient $\lambda = 50$.

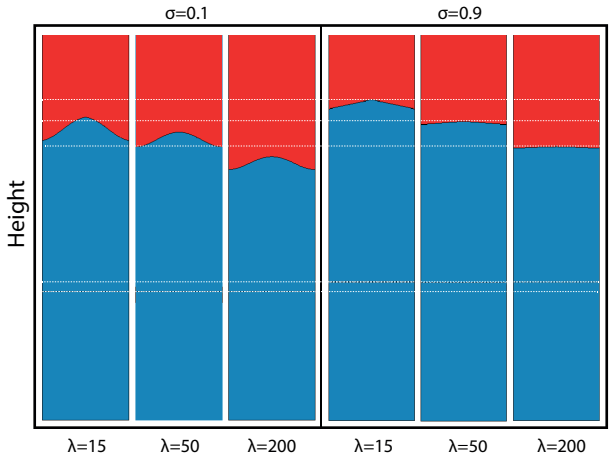

Figure 7: Numerical simulation results for different $\sigma = [0.1; 0.9]$ and $\lambda = [15; 50; 200]$ at time $t = 25$. Here density $\rho^+ = 1.1$, $\rho^- = 0.86$, viscosities $\mu^+ = 0.001$, $\mu^- = 0.01$, inlet pressure $p^+ = 10$.

9 Conclusion

In this paper, the finite element method (FEM) were used for the numerical solution of two dimensional problem for a viscoelastic filtration on the microscopic level. The results showed a direct dependence of the free-boundary propagation velocity on the surface tension and the Lame's elastic coefficient. It is worth noting the occurrence of significant artifacts with invalid values of λ and σ.

Acknowledgements

The reported study was funded by RFBR according to the research project No 18-31-00042.

References

[1] R. Cook, D. Malkus and R. Witt *Concepts and applications of finite element analysis*, John Wiley and Sons, 2001.

[2] B. Cockburn, *Discontinuous Galerkin methods*, E ZAMM Z. Angew. Math. Mech. **83** (2003) 731–754.

[3] A. Ern and J.L. Guermond, *Theory and practice of finite elements*, Springer, 2004.

[4] J. Ferziger and M. Peric *Computational methods for fluid dynamics*, Springer Berlin etc., 1999.

[5] J.F. Gerbeau and M. Vidrascu, *A quasi-Newton algorithm based on a reduced model for fluid-structure interaction problems in blood flows*, ESAIM: Math. Model. Numer. Anal. **37** (2003) 631–648.

[6] S. Gilbert and F. George, *An analysis of the finite element method*, Prentice Hall, 1973.

[7] M. Gurtin, E. Fried and L. Anand *The mechanics and thermodynamics of continua*, Cambridge Univ Print, 2009.

[8] B. Hans-Joachim and S. Michael, *Fluid-structure interaction: modelling, simulation, optimization*, Springer-Verlag, 2006.

[9] K. Izadpanah, A. Mesforush and A. Nazemi, *Stabilized IMLS based element free Galerkin method for stochastic elliptic partial differential equations*, J. Math. Model. **7** (2019) 469-496.

[10] L.J. Khaled-Abad and R. Salehi, *Weak Galerkin finite element method for an inhomogeneous Brusselator model with cross-diffusion*, J. Math. Model. **7** (2019) 277-285.

[11] D.L. Logan, *A first course in the finite element method*, Cengage Learning, 2011.

[12] A. Rodriguez, F. Agusti, P. Foguet and A. Huerta, *Arbitary Lagrangian-Eulerian (ALE) formulation for hyperelastoplasticity*, Internat. J. Numer. Methods Engrg. **53** (2002) 1765–2017.

[13] C. Roy, C. Nelson, T. Smith and C. Ober, *Verification of Euler/Navier-Stokes codes using the method of manufactured solutions*, Internat. J. Numer. Methods Fluids **44** (2004) 599–620.

[14] J.F. Sigrist, *Fluid-Structure Interaction: An Introduction to Finite Element Coupling*, Wiley, 2015.

[15] I.M. Smith, D.V. Griffiths and L. Margetts, *Programming the finite element method*, Wiley, 2014.

[16] M. Souli, A. Ouahsine and L. Lewin, *ALE formulation for fluid-structure interaction problems*, Comput. Methods Appl. Mech. Engrg. **190** (2000) 659–675.

[17] P.K. Tripathy, S.K. Mishra and A.J. Chamkha, *Simulation of particle diffusion and heat transfer in a two-phase turbulent boundary layer using the Eulerian-Eulerian approach*, J. Math. Model. **3** (2016) 169-187.

[18] J. Tu, G. Yeoh and C. Liu, *Computational fluid dynamics: a practical approach*, Butterworth Heinemann, 2008.

[19] O.C. Zienkiewicz, R.L. Taylor, J.Z. Zhu, *The Finite Element Method: Its Basis and Fundamentals*, Butterworth-Heinemann, 2013.